# Sensitive Microspectrophotometric Determination of $Dy^{3+}$, $Ho^{3+}$ and $Lu^{3+}$ with Xylenol Orange in Presence of Cetylpyridinium Bromide as a Cationic Surfactant

P. P. Kalbende[1*], S. S. Butoliya[2], A. B. Zade[3]

[1*]Department of Chemistry, Jagadamba Mahavidyalaya, Achalpur-444806, Dist.-Amravati, (MS) India.

*E-mail:- pawankalbende@gmail.com

[2]Department of Chemistry, Ramdeobaba University, Nagpur-440013, (MS) India

[3]Department of Chemistry, Laxminarayan Institute of Technology, Nagpur-440033 (MS) India

Received: 3.3.2025, Revised: 31.8.2025, 5.9.2025, 28.9.2025 Accepted: 14.10.2025

**Abstract:** Xylenol orange (XO) is known to form violet-colored binary complexes with various lanthanide ions, which have been effectively utilized for metal ion detection. When a cationic surfactant like cetylpyridinium bromide (CPB) is introduced into the XO solution at certain pH levels, a noticeable loss of color occurs. This discoloration arises from the electrostatic interaction between the anionic XO and the cationic CPB. Upon subsequent addition of specific metal ions such as $Dy^{3+}$, $Ho^{3+}$, and $Lu^{3+}$, intense, stable and water-soluble ternary complexes are generated. These complexes display significant bathochromic shifts i.e. 42 nm for $Dy^{3+}$, 44 nm for $Ho^{3+}$, and 42 nm for $Lu^{3+}$ alongside an increase in absorbance at the newly shifted wavelengths. Job's method of continuous variation revealed a stoichiometric ratio of 1:2:4 (metal ion:XO:CPB) in the formed ternary complexes. Stability constants (log K values) for both binary and ternary complexes were determined, indicating enhanced stability of the ternary complexes across a broader pH range.

The maximum absorption was observed at 612 nm for $Dy^{3+}$, and 610 nm for both $Ho^{3+}$ and $Lu^{3+}$. Further investigations included optimization of analytical parameters such as the sequence of reagent addition, reaction time and temperature, reagent concentrations, adherence to Beer's law, photometric ranges, Sandell's sensitivity, and molar absorptivity. The influence of potential interfering ions on metal ion detection was also examined. Overall, a straightforward, rapid, and highly sensitive spectrophotometric method has been developed for the determination of $Dy^{3+}$, $Ho^{3+}$, and $Lu^{3+}$ using xylenol orange.

**Keywords:** Spectrophotometry, Xylenol Orange (XO), Cetylpyridinium bromide (CPB), Lutetium ($Lu^{3+}$), Dysprosium ($Dy^{3+}$), Holmium ($Ho^{3+}$).

## 1. Introduction

Microdetermination of rare earth elements, particularly lanthanides such as $Dy^{3+}$, $Ho^{3+}$ and $Lu^{3+}$ has attracted increasing attention owing to their critical roles in lasers, nuclear reactors, phosphors, magnetic materials, and medical diagnostics. As industrial usage of rare earth elements increases, their accurate quantification in environmental, geological and biological samples becomes essential. However, the analytical determination of lanthanides presents considerable challenges owing to their similar chemical behaviors and low natural abundance[1-7]. Thus, the development of sensitive, selective, and cost-effective spectrophotometric methods remains an ongoing necessity. In recent times, spectrophotometric methods have gained significant attention as effective tools for the selective identification of metal ions, owing to their ease of use, high sensitivity and suitability for analyzing small sample volumes.

Microspectrophotometry, a compact and highly sensitive refinement of traditional UV-visible spectrophotometry, has proven to be an effective technique for detecting metal ions at trace levels[8]. Its enhanced sensitivity, coupled with low sample volume requirements, makes it particularly suitable for rare earth element detection in microscale and complex matrices. In this context, the complexation of lanthanides with chromogenic ligands forms the foundation for spectrophotometric detection. Among such ligands, Xylenol Orange (XO) has proven to be an effective metallochromic indicator due to its high chelating ability and strong color development upon metal complexation[9].

Xylenol Orange (XO), a polycarboxylic acid dye, forms strongly colored complexes with lanthanides in mildly acidic to neutral media, enabling their spectrophotometric detection. Binding with lanthanides shifts XO's absorption maximum, allowing quantitative estimation. Sensitivity and selectivity can be enhanced using surfactants, which form micelles that concentrate and stabilize metal–ligand complexes. In this study, the cationic surfactant cetylpyridinium bromide (CPB) is used to improve detection of $Dy^{3+}$, $Ho^{3+}$, and $Lu^{3+}$. CPB interacts with XO and its metal complexes, pre-concentrating analytes within micelles, increasing molar absorptivity, lowering detection limits, and sharpening absorption bands for enhanced analytical performance[10, 11].

Xylenol Orange (XO), forms stable complexes with lanthanides, previous works have demonstrated the utility of micellar systems in spectrophotometric and fluorimetric determinations of metal ions. For example, Sharma and Garg[12] have reported improved

sensitivity for $Fe^{3+}$ and $Al^{3+}$ in the presence of cetyltrimethylammonium bromide (CTAB), while Goyal et al.[13] highlighted the role of micelles in suppressing interference effects in multi-metal systems. The sensitivity and selectivity of metal–xylenol orange complexes can be enhanced using surfactants, which modify complexation conditions and improve analyte distribution within micelles[14]. Bai et al. reported improved detection limits and analytical performance for various metal ions using XO as a chromogenic agent[15]. Tian et al. demonstrated that cetylpyridinium bromide (CPB) increases the stability and sensitivity of metal–XO complexes[16]. Gupta et al. highlighted XO's effectiveness in environmental analysis, emphasizing pH-dependent selectivity for heavy metals[17], while Bhatt et al. showed that surfactant choice significantly influences complexation behavior and detection sensitivity[18].

Reynolds et al compares Xylenol Orange with other chromogenic reagents, detailing its advantages in forming stable and detectable complexes with a range of metal ions. The study emphasizes the reagent's selectivity and practical applications in microspectrophotometry[19]. Neodymium present in mixed rare earth samples has been successfully quantified using a spectrophotometric technique involving semi-xylenol orange and cetylpyridinium chloride[20]. Similarly, several rare earth elements such as samarium, dysprosium, yttrium, gadolinium, neodymium, praseodymium, lanthanum, and cerium have been analyzed using xylenol orange in combination with CPB through spectrophotometric methods[21]. Additionally, the use of flow injection analysis coupled with spectrophotometry has been employed for the determination of rare earth elements, utilizing their interaction with xylenol orange in the presence of CPB[22].

Fluoride has been determined spectrophotometrically using an aluminium–xylenol orange complex[23], and Primo reported the estimation of lanthanum(III) and other rare earths with xylenol orange[24]. Dhepe et al. developed a micro-level method for gadolinium(III) and terbium(III) using xylenol orange with cetylpyridinium bromide (CPB)[25], while Jimmy et al. compared the determination of neodymium(III), praseodymium(III), samarium(III), and terbium(III) in aqueous and micellar media[26]. However, the role of CPB in spectrophotometric determination of heavy lanthanides such as $Dy^{3+}$, $Ho^{3+}$, and $Lu^{3+}$ remains unexplored. This study addresses the gap by optimizing conditions for complex formation, including pH, reagent and surfactant concentrations, and reaction time.

This study is designed to develop a sensitive method for micro-level determination of selected metal ions. Unlike conventional spectrophotometry, microspectrophotometric techniques combined with micellar enhancement enable trace detection in biological fluids, wastewater,

and mineral extracts, while being eco-friendly, cost-effective, and accessible compared to instruments like ICP-MS or AAS. The method emphasizes green chemistry by reducing reagent use and waste. Validation will be carried out through parameters such as linearity, detection limits, reproducibility, selectivity, interference studies, and application to real samples, ensuring accuracy and practical utility.

The present study investigates the sensitive determination of $Dy^{3+}$, $Ho^{3+}$, and $Lu^{3+}$ using microspectrophotometry with Xylenol Orange in the presence of cetylpyridinium bromide (CPB). CPB enhances molar absorptivity, solubility, and stability of the metal–XO complexes, enabling more robust detection. The research focuses on optimizing complex formation conditions, evaluating stability, and assessing analytical performance, including detection limits, sensitivity, and precision. By combining micellar enhancement with microanalytical techniques, this approach offers a rapid, reproducible, and eco-friendly method for lanthanide quantification, with applications in environmental, material, and pharmaceutical analysis.

## 2. Experimental:

All chemicals employed in this study were of analytical reagent grade. Xylenol Orange (XO) was procured from Sigma Chemical Company (USA), while cetylpyridinium bromide (CPB) was obtained from Aldrich Chemical Company. The purity of CPB was verified through argentometric titration to determine its bromide ion content. Lanthanide elements were used in the form of their oxides, supplied by Indian Rare Earths Ltd., India, without any further purification.

Stock solutions of XO ($1 \times 10^{-2}$ M) and CPB ($1 \times 10^{-1}$ M) were prepared using double-distilled water. A $1 \times 10^{-2}$ M solution of lanthanide (III) ions was obtained by dissolving the respective metal oxides in a small quantity of AR-grade hydrochloric acid. The lanthanide solutions were standardized by precipitating the metal ions as oxalates, followed by volumetric estimation using bromopyrogallol red as the complexometric indicator[27]. Further dilutions to achieve the required concentrations were made with double-distilled water. In the experimental procedure, CPB solution was added first to the XO solution and left undisturbed for 30 minutes to promote interaction. Subsequently, the lanthanide ion solution was introduced and also left for 30 minutes to attain equilibrium. This order of addition was maintained throughout all experiments. A series of solution sets was prepared by pipetting appropriate volumes of XO solution at a concentration of $1 \times 10^{-3}$ M into 25 mL volumetric flasks. For recording the absorption spectra, the final concentrations of XO and CPB were adjusted to $2.0 \times 10^{-5}$ M and $2.0 \times 10^{-4}$ M, respectively.

Absorbance readings were recorded on a Systronics Visiscan-167 spectrophotometer using matched glass cuvettes with a 10 mm path length and powered by a 220V supply. pH measurements were made using an Elico Model LI–10 pH meter fitted with a combined glass and calomel electrode, which was regularly calibrated with standard buffer solutions (potassium hydrogen phthalate, pH 4.02; and borax). Adjustments to the pH were made using suitable concentrations of hydrochloric acid and sodium hydroxide solutions.

## 3. Result and Discussion:

### 3.1 Absorption Spectra of XO

To examine the absorption behavior of XO in the presence of CPB, different XO:CPB molar ratios (1:1, 1:10, and 10:1) were prepared using stock solutions of XO ($1 \times 10^{-3}$ M) and CPB ($1 \times 10^{-2}$ M). It was found that the 1:10 ratio of XO to CPB was essential for observing the decolorization effect, and hence, CPB was used in tenfold excess over XO in the current investigations. For brevity, only the graphs corresponding to the 1:10 ratio are presented. The wavelengths of maximum absorbance ($\lambda_{max}$) in both the absence and presence of CPB are summarized in Table 1[28, 29]. The absorption spectra of XO were studied across a pH range of 1.0 to 10.0 in the visible region (400–700 nm), both without and with CPB in the figure 1 (A and B) respectively. The color of XO was observed to vary with pH. The $\lambda_{max}$ values of XO at different pH levels, with and without CPB, are listed in Table 1.

**Table 1** $\lambda_{max}$ of XO in absence and presence of CPB at different pH

| XO | | XO + CPB | |
|---|---|---|---|
| **pH** | **$\lambda_{max}$** | **pH** | **$\lambda_{max}$** |
| 1.0 | 446 | 1.0 | 456 |
| 2.0 | 450 | 2.0 | 460 |
| 3.0 | 426 | 3.0 | 442 |
| 3.5 | 450 | 3.5 | 442 |
| 4.0 - 7.0 | 452 | 4.0 - 7.0 | 448 |
| 7.5 - 10.0 | 618 | 7.5 - 10.0 | 626 |

The findings of this study indicate that Xylenol orange (XO) exhibits the highest decolorization at pH 9.0 when CPB is present, whereas in acidic conditions, maximum decolorization occurs around pH 6.0. In the absence of CPB, XO shows an absorbance of 0.458 at its $\lambda_{max}$ of 618 nm at pH 9.0. In contrast, when CPB is present at the same pH, the absorbance decreases to 0.296 at a slightly shifted $\lambda_{max}$ of 626 nm. The findings indicate that

CPB causes a decrease in the absorbance of XO, with this effect being more significant under alkaline conditions compared to acidic environments. The absorption spectra of XO and XO + CPB are shown in Fi.1.

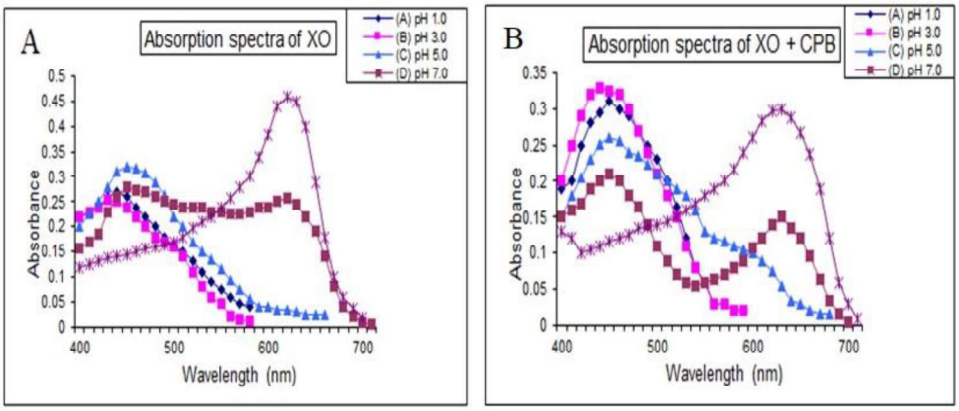


**Fig. 1** Absorption spectra of A) XO B) XO + CPB

### 3.2 Composition of XO - Surfactant Complex

The influence of different concentrations of CPB on the absorbance of Xylenol Orange (XO) was examined at pH 6.0 ($\lambda_{max}$ 452 nm, acidic medium) and at pH 9.0 ($\lambda_{max}$ 618 nm, alkaline medium) to determine the stoichiometric composition of the XO-CPB complex. For this purpose, three distinct concentrations of XO were employed to investigate the composition of the XO-CPB complex, as outlined below.

Curve A- 3.0 x $10^{-5}$ M, Curve B- 2.7 x $10^{-5}$ M, Curve C- 2.33 x $10^{-5}$ M

The effect of diverse CPB concentration on the absorbance of XO at pH 6.0 and pH 9.0 is illustrated in Figs. 2 A and B, respectively. The curves labeled A, B, and C display two distinct regions. The initial descending segment of each curve reflects a nearly linear decrease in absorbance as the CPB concentration increases. Beyond this, the curves level off, forming an extended horizontal section where no noteworthy change in XO absorbance is noticed, even with the addition of a large excess of CPB. The graphs clearly indicate that the utmost decolorization effect is achieved at an XO:CPB molar ratio of 1:2. Once this ratio is reached, further addition of CPB even up to ten times excess does not affect the absorbance of XO. The resulting complex can be tentatively represented as $[XO(CPB)_2]$. Similar findings for XO and CPB interactions have also been reported in earlier studies[30, 31].

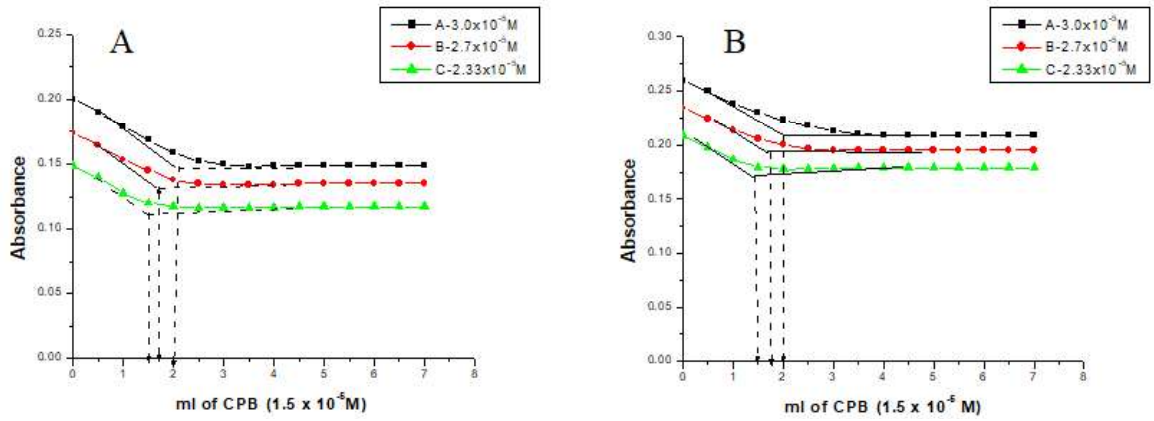


**Fig. 2** A) Influence of CPB on XO at pH 6.0 and $\lambda_{max}$ 452 nm.

B) Influence of CPB on XO at pH 9.0 and $\lambda_{max}$ 618 nm.

### 3.3 Absorption Spectra of some lanthanides ($Dy^{3+}$, $Ho^{3+}$ and $Lu^{3+}$) with XO in absence and presence of CPB

The absorption spectra of XO, XO+CPB, XO+lanthanide metal ions ($Dy^{3+}$, $Ho^{3+}$ and $Lu^{3+}$) and XO+CPB+lanthanide metal ions ($Dy^{3+}$, $Ho^{3+}$ and $Lu^{3+}$) have been studied in the pH range 1.0 to 10.0 keeping the ratio of metals: XO: CPB, 1:1:10 and 4:1:10 in the entire visible region. A comparative absorption spectral values of ($Dy^{3+}$, $Ho^{3+}$ and $Lu^{3+}$) for XO, XO+CPB, XO+ lanthanide and XO+CPB+ lanthanides in the pH range 1.0-10.0 with a difference of 0.5 or less pH units and graphically shown in Fig. 3 (a-d) at pH 6.0. The concentration of various reactants used for the spectral measurements are as follows.

i. Final concentration of XO - $2.0 \times 10^{-5}$ M
ii. Final concentration of CPB - $2.0 \times 10^{-4}$ M
iii. Final concentration of lanthanide metals- $6.0 \times 10^{-5}$ M

The absorption maxima of XO and its complexes with lanthanides, both in the absence and presence of CPB, at various pH levels. The absorption spectrum of XO exhibits a peak at 452 nm within the pH range of 3.5 to 7.0, and at 618 nm between pH 7.5 and 9.0. In the presence of CPB, the λmax of XO is observed around 442 nm at pH 3.0–3.5, shifts to 448 nm between pH 4.0 and 7.0, and appears at 626 nm in the pH range of 7.5 to 9.0.

The binary complexes of lanthanide ions exhibited $\lambda_{max}$ in the range of **566–570 nm** within **pH 4.5–6.4**, accompanied by a broad peak indicating complex formation with a change in color and $\lambda_{max}$ shift. In contrast, the ternary complexes showed $\lambda_{max}$ in the **540–580 nm** range at **pH 3.5–4.5**, which gradually shifted toward **620 nm** as pH increased from **5.0 to 9.0**. This

peak became sharper and more intense, with a marked increase in absorbance up to **pH 6.5**, confirming stronger ternary complex formation.

A critical studies of absorption spectra of lanthanide complexes with XO show a broad peak in the pH range 4.5 to 6.4 indicating the formation of binary complex showing the $\lambda_{max}$ 570 nm for Dy(III), 566 nm for Ho(III), and 568 nm for Lu(III) at pH 6.0. The curve shows poor complexation in the pH range 3.0 to 4.0. Thus, binary complexation takes place with bathochromic shift 118 nm, 114 nm and 116 nm for Dy(III), Ho(III) and Lu(III) respectively. A single well-defined absorption band was observed for each metal complex in the presence of CPB, with $\lambda_{max}$ at 612 nm for Dy(III), and at 610 nm for both Ho(III) and Lu(III).

A substantial bathochromic shift in $\lambda_{max}$ was observed upon addition of CPB, accompanied by increased absorbance at the shifted wavelength, confirming stronger complexation compared to the binary system. The net shift between binary and ternary complexes was **42 nm for Dy(III), 44 nm for Ho(III), and 42 nm for Lu(III)**, with higher absorbance values indicating enhanced molar absorptivity. Comparison of absorption spectra of the free reagent and its lanthanide complexes revealed optimal complex formation at **pH 6.1 (Dy), pH 6.2 (Ho), and pH 6.0 (Lu)**. The absorption spectra (Figure 3a–d) further confirm the ternary complex formation, showing bathochromic shifts of **160 nm for Dy(III)** and **158 nm for both Ho(III) and Lu(III)**.

In Fig. 3(a–d), **Curve A** represents the absorption spectrum of XO alone, while **Curve B** shows XO in the presence of CPB. The spectra of the **binary lanthanide complexes** are presented in **Curve C**, and **Curve D** corresponds to the **ternary complexes**. A distinct bathochromic shift is evident, with $\lambda_{max}$ shifting by approximately **118 nm** for binary complex formation (without CPB) and by about **160 nm** for ternary complex formation (with CPB). The $\lambda_{max}$ values and their corresponding shifts are summarized in **Table 2**.

It was further observed that the **ternary complexes exhibited higher absorbance values at their $\lambda_{max}$ compared to the binary complexes**, resulting in a corresponding increase in molar absorptivity. The intense blue-colored ternary complexes thus not only showed a pronounced **bathochromic shift** but also a **substantial enhancement in absorbance** in the

presence of CPB, clearly demonstrating the sensitization of the color reactions[32–34].

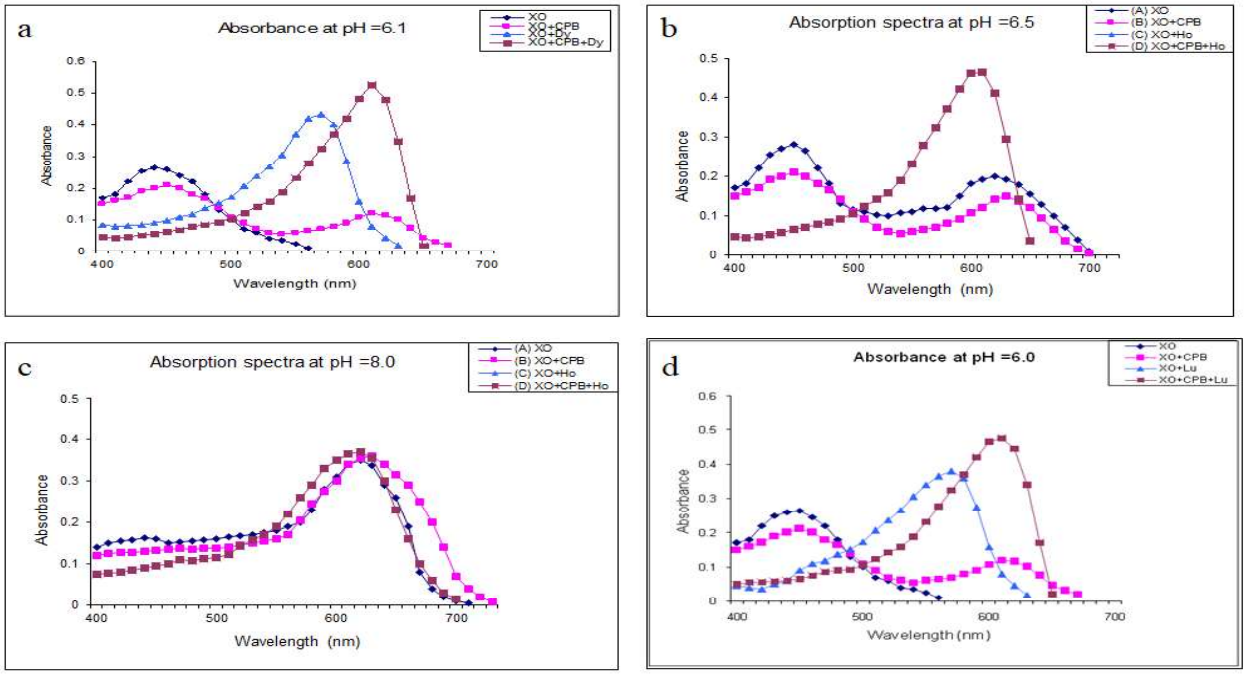


**Fig. 3 (a-d):** Absorption spectra of XO at a) pH 6.1 for Dy (III) b) pH 6.5 for Ho (III) c) 8.0 for Ho (III) d) pH 6.0 for Lu (III)

**Table 2 Absorbance maximum and Bathochromic shift of lanthanide complexes of XO in absence and presence of CPB.**

| Lanthanide complexes | $\lambda_{max}$ of XO (nm) | | $\lambda_{max}$ of complexes (nm) | | Bathochromic shift as compared to reagent (nm) | | Bathochromic shift between binary and ternary complex (nm) |
|---|---|---|---|---|---|---|---|
| | Absence | Presence | Absence | Presence | Absence | Presence | |
| Dy (III) | 452 | 448 | 570 | 612 | 118 | 160 | 42 |
| Ho (III) | 452 | 448 | 566 | 610 | 114 | 158 | 44 |
| Lu (III) | 452 | 448 | 568 | 610 | 116 | 158 | 42 |

### 3.4 Effect of pH and pH range of stability

The effect of pH on the $\lambda_{max}$ values of lanthanide–XO complexes, with and without CPB, was studied over pH 1.0–10.0 and shown in Figs. 4 (a, b), 5 (c, d) and 6 (e, f).The XO reagent displayed constant $\lambda_{max}$ at 452 nm (pH 3.5–7.0) and 618 nm (pH 7.5–9.0), while in the presence of CPB, these shifted to 448 nm and 626 nm, respectively. Binary lanthanide complexes (curve C) remained stable between pH 4.5–6.4, whereas ternary complexes with CPB (curve D) showed a bathochromic shift and stability between pH 5.0–7.0 (Table 3).

Absorbance variations with pH are illustrated in Figs 4–6 for Dy(III), Ho(III), and Lu(III), showing $\lambda_{max}$ at 570/612 nm, 566/610 nm, and 568/610 nm for binary/ternary complexes, respectively. In ternary systems, absorbance increased linearly with pH, then plateaued, remaining constant within the stability range. The optimum pH for stable complex formation was ~5.6–6.4 with CPB and ~5.8–6.4 without CPB[35–37].

**Table 3:** pH range of stability of lanthanide complexes of XO in absence and presence of CPB.

| Lanthanide complexes | $\lambda_{max}$ of complexes (nm) | | pH range of stability of constant wavelength (nm) | | pH range of stability of constant absorbance | |
|---|---|---|---|---|---|---|
| | Absence | Presence | Absence | Presence | Absence | Presence |
| Dy (III) | 570 | 612 | 4.5 – 6.4 | 5.0 – 7.0 | 5.9 – 6.4 | 5.6 – 6.4 |
| Ho (III) | 566 | 610 | 4.5 – 6.2 | 5.0 – 7.0 | 5.6 – 6.2 | 5.6 – 6.4 |
| Lu (III) | 568 | 610 | 4.5 – 6.2 | 5.0 – 7.0 | 5.7 – 6.2 | 5.7 – 6.4 |

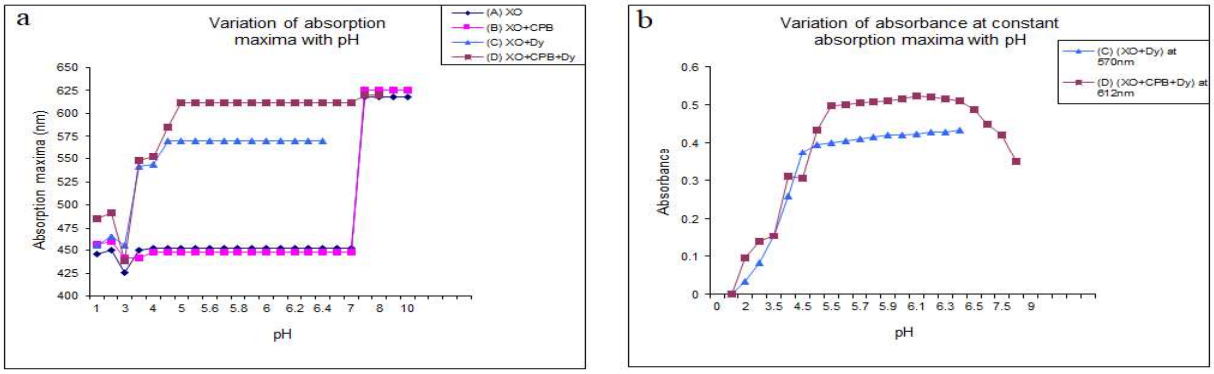


**Fig. 4 (a):** Variation of absorption maxima with pH for Dy(III).
**Fig. 4 (b):** Variation of absorbance at constant absorption maxima with pH for binary and ternary complex of Dy(III) with XO.

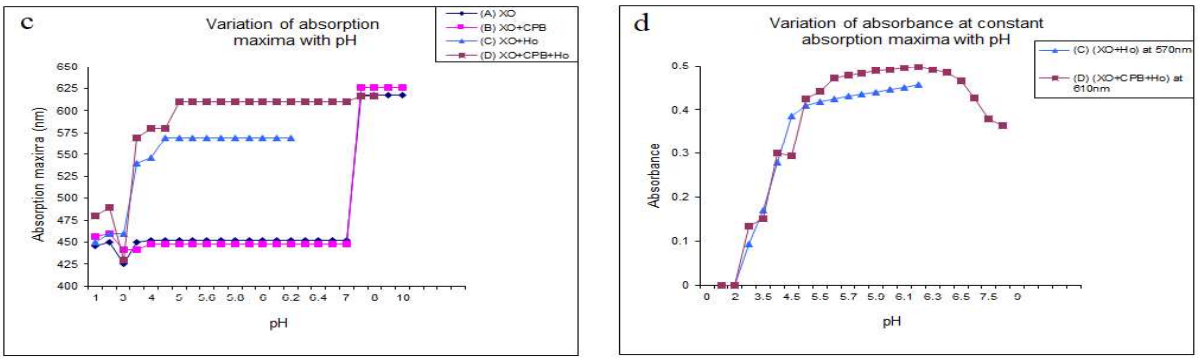


**Fig. 5 (c):** Variation of absorption maxima with pH for Ho(III).
**Fig. 5 (d):** Variation of absorbance at constant absorption maxima with pH for binary and ternary complex of Ho(III) with XO.

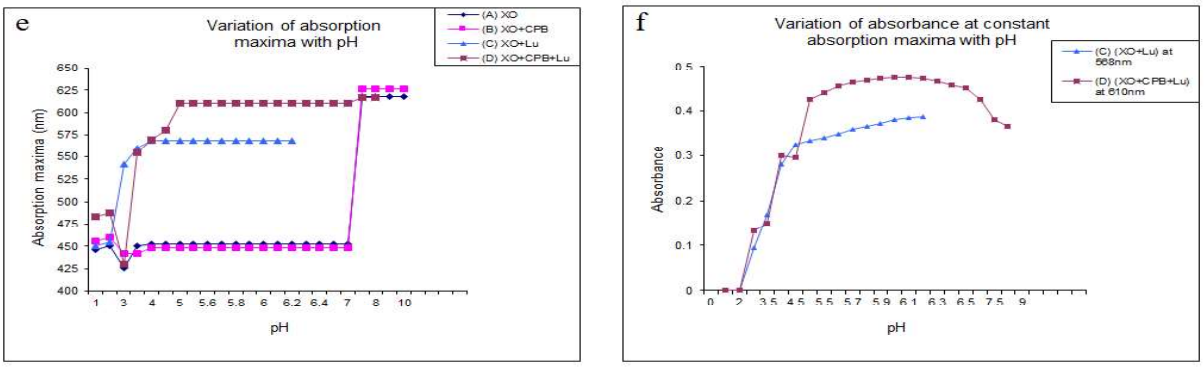


**Fig. 6 (e):** Variation of absorption maxima with pH for Lu(III).

**Fig. 6 (f):** Variation of absorbance at constant absorption maxima with pH for binary and ternary complex of Lu(III) with XO.

### 3.5 Composition and log K values of Complexes

The composition of lanthanide complexes was determined by Job's method of continuous variation. Spectral analysis showed maximum complex formation at specific pH and absorbance wavelengths, both with and without the surfactant CPB. Equimolar solutions of lanthanide ions and XO were mixed in a constant total volume of 25 mL, with or without CPB, and absorbance was recorded by varying reactant proportions.

To investigate the composition in absence of CPB, three different equimolar concentrations ($2.5 \times 10^{-4}$ M, $1.66 \times 10^{-4}$ M, $1.25 \times 10^{-4}$ M) were employed for the formation of complexes between XO and the lanthanide ions. These studies indicated a composition of 1:2 (lanthanide:XO) for the binary complexes. Specifically, the concentrations used were for Dy(III) at pH 6.4 with $\lambda_{max}$ 570 nm, Ho(III) at pH 6.2 with $\lambda_{max}$ 566 nm, and Lu(III) at pH 6.2 with $\lambda_{max}$ 568 nm, as represented in Figs. 7(a), 8(c), and 9(e), respectively. Figs. 7(b), 8(d), and 9(f) illustrate the plots obtained for the composition studies conducted in presence of CPB at varying concentrations. These curves represent the complex formation between XO and the lanthanide ions under investigation: Dy(III) at pH 6.1 with $\lambda_{max}$ 612 nm, Ho(III) at pH 6.2 with $\lambda_{max}$ 610 nm, and Lu(III) at pH 6.0 with $\lambda_{max}$ 610 nm. The results indicate that the composition of the ternary complexes is 1:2:4 (metal:XO:CPB).

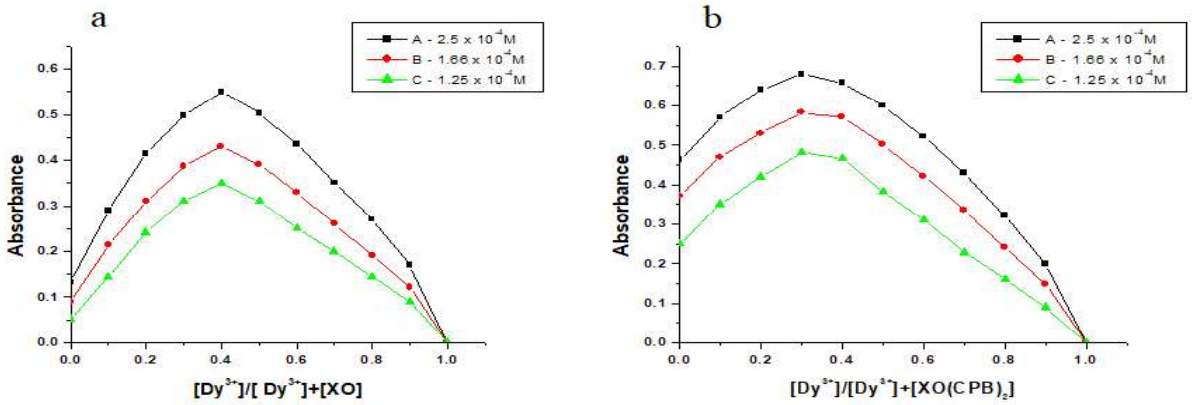


**Fig. 7 (a)** Curves of Job's method of binary complex show composition of Dy: XO as 1:2 at pH 6.4 and $\lambda_{max}$ 570nm

**Fig. 7 (b)** Curves of Job's method of ternary complex show composition of Dy: XO: CPB as 1:2:4 at pH 6.1 and $\lambda_{max}$ 612 nm

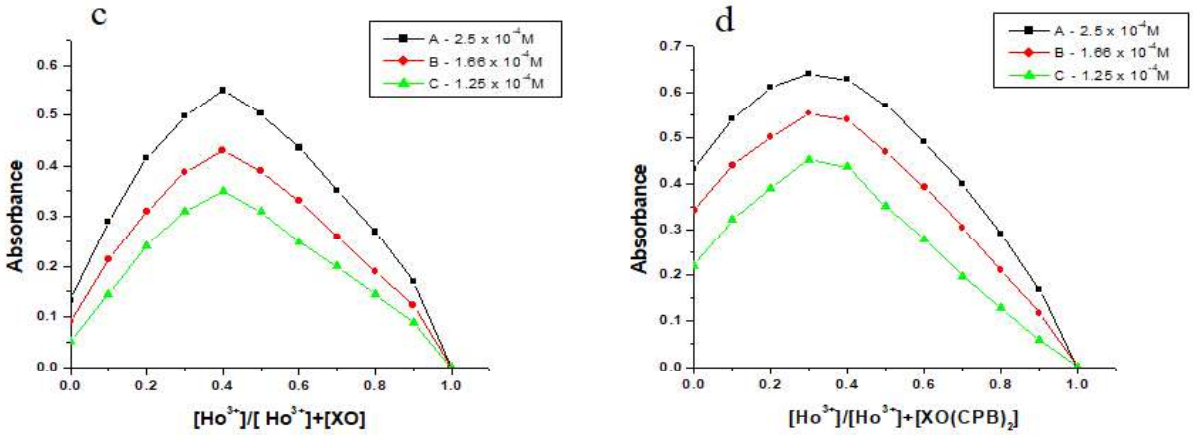


**Fig. 8 (c)** Curves of Job's method of binary complex show composition of Ho: XO as 1:2 at pH 6.2 and $\lambda_{max}$ 566 nm

**Fig. 8 (d)** Curves of Job's method of ternary complex show composition of Ho: XO: CPB as 1:2:4 at pH 6.2 and $\lambda_{max}$ 610nm

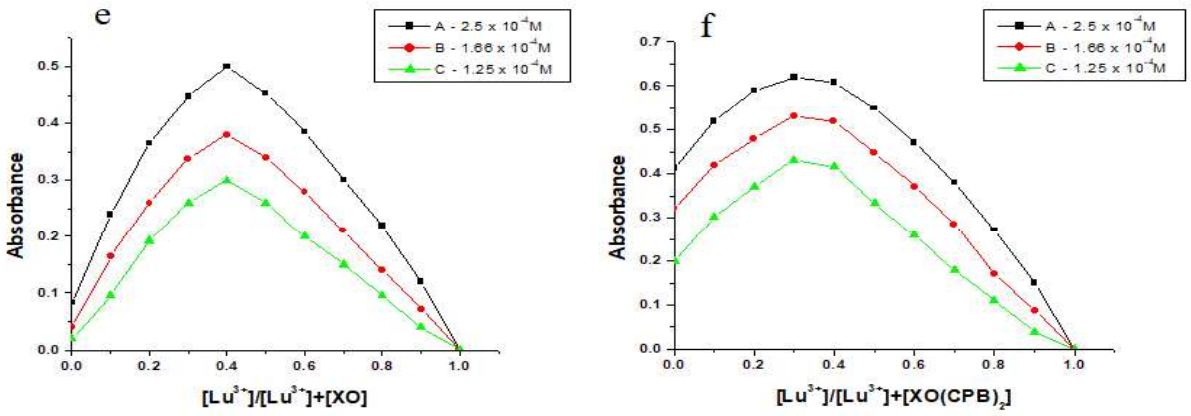


**Fig. 9 (e)** Curves of Job's method of binary complex show composition of Lu: XO as 1:2 at pH 6.2 and $\lambda_{max}$ 568 nm

**Fig. 9 (f)** Curves of Job's method of ternary complex show composition of Lu: XO: CPB as 1:2:4 at pH 6.0 and $\lambda_{max}$ 610 nm

The compositions of the complexes formed between lanthanide metal ions and XO, as determined by Job's method of continuous variation, are summarized in Tables 5 and 6 for studies conducted in the absence and presence of CPB, respectively[38, 39]. The stoichiometric ratio of lanthanide ions to XO was found to be 1:2 in both cases, aligning well with previously reported findings[40, 41]. Therefore, in the presence of CPB, the composition of the lanthanide complexes can be represented as $M[XO(CPB)_2]_2$, corresponding to a metal:XO:CPB ratio of 1:2:4. The formation of this complex may be expressed as:

$$M + 2[XO(CPB)_2] \rightleftharpoons M[XO(CPB)_2]_2$$

The stability constants (log K values) of the XO complexes were evaluated from the Job's plots and are reported in Tables 5 and 6 for the absence and presence of CPB, respectively. It was observed that the ternary complexes exhibit higher stability than the binary complexes. This enhanced stability is likely due to the binding of two cationic CPB molecules to the anionic XO, forming a modified reagent $XO(CPB)_2$ that stabilizes the resulting complex. The cationic micellar environment provided by CPB further contributes to this stabilization. The results also indicate that, without CPB, the log K values increase from $Gd^{3+}$ to $Lu^{3+}$, whereas in the presence of CPB, the log K values decrease across this series. This trend may be attributed to the steric hindrance caused by the bulky cationic surfactant molecules, which can affect complexation, particularly with smaller lanthanide ions that result from lanthanide contraction[42].

**Table 4:** Composition and stability constants of XO complexes in absence of CPB.

| Complexes of XO | pH of study | $\lambda_{max}$ of study | Composition M:XO | log K values by Job's method |
|---|---|---|---|---|
| Dy (III) | 6.4 | 570 | 1:2 | 5.44 |
| Ho (III) | 6.2 | 566 | 1:2 | 5.48 |
| Lu (III) | 6.2 | 568 | 1:2 | 5.52 |

**Table 5:** Composition and stability constants of XO complexes in presence of CPB.

| Complexes of XO | pH of study | $\lambda_{max}$ of study | Composition $M:[XO:(CPB)_2]_2$ | log K values by Job's method |
|---|---|---|---|---|
| Dy (III) | 6.1 | 612 | 1:2:4 | 8.56 |
| Ho (III) | 6.2 | 610 | 1:2:4 | 8.48 |
| Lu (III) | 6.0 | 610 | 1:2:4 | 8.02 |

### 3.6 Analytical applications of Xylenol Orange complex of lanthanides in presence of Cetylpyridinium Bromide

#### 3.6.1 Order of Addition of Reactants

The sequence in which the reactants are added plays a crucial role and must be carefully maintained throughout the experiments. In all studies, the CPB solution was first introduced into the XO solution. The mixture was subsequently left undisturbed for a minimum of 30 minutes to allow full equilibration and facilitate the formation of the XO–CPB complex. Only after this equilibration period was the metal ion solution added to facilitate the formation of ternary complex. Adhering to this specific order of addition is essential for obtaining the desired ternary complex. Any deviation or reversal of this sequence can lead to the formation of alternative complexes, resulting in irreproducible data[43].

#### 3.6.2 Effect of Time and Temperature on the Stability of Complex Color

To study the effect of time and temperature on the stability of the complex color, the CPB solution was first combined with the XO solution and left for at least 30 minutes to ensure complete decolorization. Following this, the lanthanide ion solution was added to the treated reagent to allow complex formation. The final mixture, containing $2.0 \times 10^{-5}$ M XO, $2.0 \times 10^{-4}$ M CPB, and $2.0 \times 10^{-5}$ M lanthanide ion, was adjusted to pH 6.0. The color of the complex developed almost instantly upon mixing. Absorbance was recorded at regular time intervals at the $\lambda_{max}$ of each complex, and the readings remained stable even after 12 hours,

indicating remarkable stability over time. Furthermore, the absorbance values of the ternary complex were unaffected by temperature variations between 20°C and 60°C, confirming that the color intensity was not influenced within this temperature range[44].

### 3.6.3 Effect of Reagent Concentration on Color Development

A ten-fold excess of CPB was added to varying concentrations of $2.0 \times 10^{-5}$ M XO solution, and the mixture was left undisturbed for at least 30 minutes to ensure complete decolorization. After this period, 1 mL of $2.0 \times 10^{-5}$ M metal ion solution was added to the modified reagent mixture. The total volume was then made up to 25 mL with distilled water at the desired pH. The absorbance of the resulting ternary complex was measured at its $\lambda_{max}$. The findings revealed that, for all metal ions examined, the concentration of XO needed to be at least double that of the metal ion to produce maximum color intensity. However, in the absence of CPB, achieving full color development required at least five times the amount of XO compared to the metal ion[45].

### 3.6.4 Beer's Law and Effective Photometric Ranges

The linearity between absorbance and metal ion concentration was assessed by varying the volume of $2.0 \times 10^{-4}$ M metal ion solution, both with and without CPB. In these experiments, XO and CPB were used at concentrations of $5.0 \times 10^{-4}$ M and $5.0 \times 10^{-3}$ M, respectively, with 2.0 mL of each reagent. The final volume was adjusted to 25 mL at the appropriate pH for each system. Absorbance was measured at the $\lambda_{max}$ corresponding to the binary and ternary lanthanide complexes formed during the study.

For Ho(III), the absorbance versus metal ion concentration plots are illustrated in Fig. 10(a) at pH 6.2 ($\lambda_{max}$ 566 nm) for the binary complex, and Fig. 10(b) at pH 6.2 ($\lambda_{max}$ 610 nm) for the ternary complex in the presence of CPB. From these plots, the Beer's law range for Ho(III) was determined to be 0.65–12.37 ppm for the binary complex and 0.51–8.36 ppm for the ternary complex. Similar investigations were conducted for Dy(III) at pH 6.4 ($\lambda_{max}$ 570 nm) in the absence of CPB, and at pH 6.1 ($\lambda_{max}$ 612 nm) in its presence; and for Lu(III) at pH 6.2 ($\lambda_{max}$ 568 nm) in the absence of CPB, and at pH 6.0 ($\lambda_{max}$ 610 nm) in the presence of CPB. The graphical data for these studies are not included here for brevity, but the Beer's law ranges are summarized in Table 6 (absence of CPB) and Table 7 (presence of CPB)[46–48].

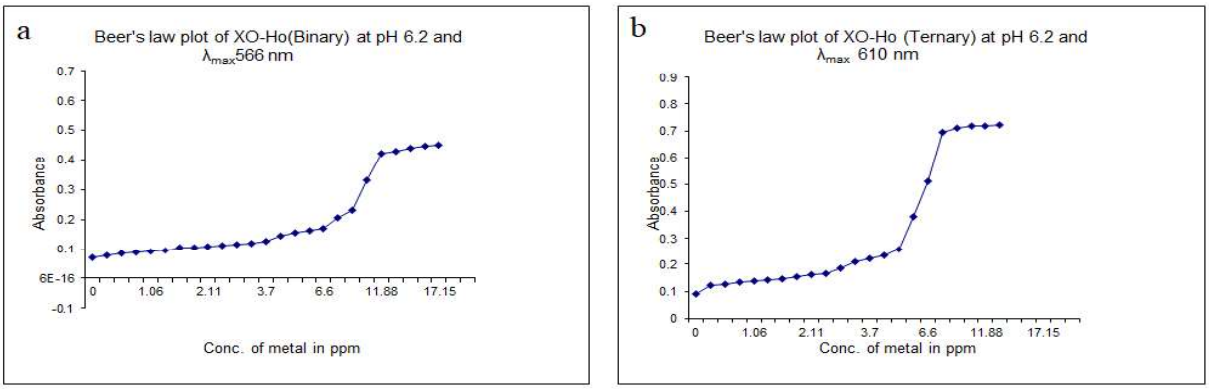


**Fig. 10 (a):** Beer's law plot of XO-Ho (Binary) at pH 6.2 and $\lambda_{max}$ 566nm.

**Fig. 10 (b):** Beer's law plot of XO-Ho (Ternary) at pH 6.2 and $\lambda_{max}$ 610 nm.

The most suitable photometric ranges were obtained from the straight-line portions of the Ringbom plots, where log metal ion concentration was plotted against % transmittance. As shown in Fig. 11(a) and 11(b) for Ho(III), the range without CPB is 1.28–6.63 ppm, while with CPB it narrows to 1.02–4.09 ppm. Similar trends were observed for the other lanthanide ions studied.

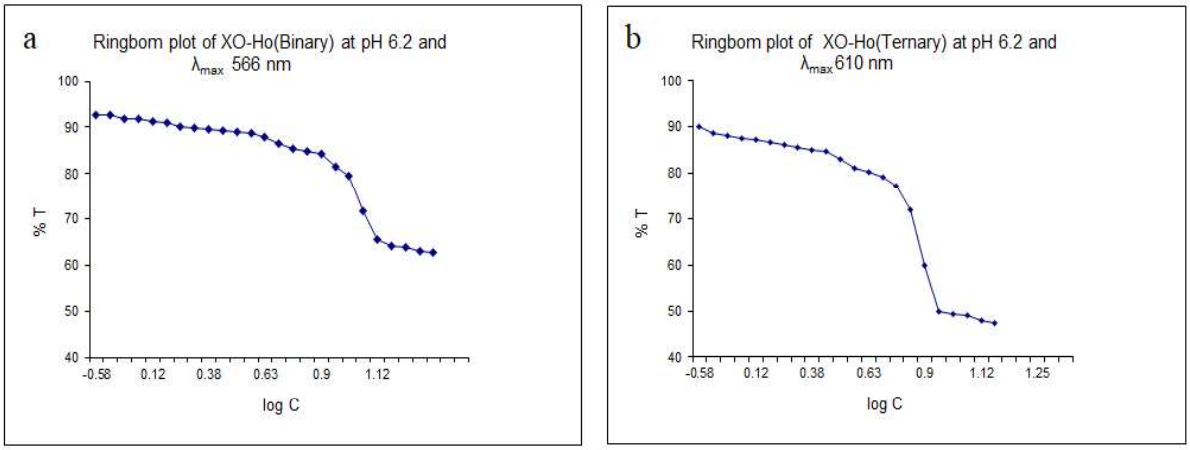


**Fig. 11 (a):** Ringbom plot of XO-Ho (Binary) at pH 6.2 and $\lambda_{max}$ 566 nm

**Fig. 11 (b):** Ringbom plot of XO-Ho (Ternary) at pH 6.2 and $\lambda_{max}$ 610 nm

The photometric ranges determined in this study are in good agreement with previously reported values for certain lanthanides[50]. This confirms that the proposed method is suitable for the determination of the studied lanthanide ions even at low concentrations. The Beer's law ranges and corresponding effective photometric ranges for these lanthanide complexes, both in the absence and presence of CPB, are summarized in Table 6 and 7 respectively.

**Table 6:** Photometric determination of Xylenol Orange complexes in absence of Cetylpyridinium bromide.

| Complexes of XO | pH of study | Wavelength of study | Beer's law ranges (ppm) | Effective photometric ranges (ppm) | Molar absorptivities ($dm^3$ $mol^{-1}$ $cm^{-1}$) | Sandell's sensitivity µg/$cm^2$ | Related Reference |
|---|---|---|---|---|---|---|---|
| Dy (III) | 6.4 | 570 | 0.64 – 12.26 | 1.26 – 6.55 | 42200 | 0.0054 | 32 |
| Ho (III) | 6.2 | 566 | 0.65 – 12.37 | 1.28 – 6.63 | 42600 | 0.0056 | 33 |
| Lu (III) | 6.2 | 568 | 0.67 – 12.48 | 1.30 – 6.74 | 41800 | 0.0064 | 36 |

**Table 7:** Photometric determination of Xylenol orange complexes in presence of Cetylpyridinium bromide

| Complexes of XO | pH of study | Wavelength of study | Beer's law ranges (ppm) | Effective photometric ranges (ppm) | Molar absorptivities ($dm^3$ $mol^{-1}$ $cm^{-1}$) | Sandell's sensitivity µg/$cm^2$ | Related Reference |
|---|---|---|---|---|---|---|---|
| Dy (III) | 6.1 | 612 | 0.58 – 08.29 | 1.01 – 4.03 | 54300 | 0.0048 | 47 |
| Ho (III) | 6.2 | 610 | 0.51 – 08.36 | 1.02 – 4.09 | 55200 | 0.0045 | 48 |
| Lu (III) | 6.0 | 610 | 0.56 – 08.00 | 1.12 – 4.75 | 54100 | 0.0044 | 49 |

### 3.6.5 Molar Absorptivity and Sensitivity of the Complexes:

The molar absorptivities of the complexes were evaluated by keeping the concentration of the reagent (XO) constant while varying the concentration of metal ions. In each case, a tenfold excess of CPB was added prior to the addition of the metal ion, and the solution was adjusted to the appropriate pH. Absorbance measurements were taken at the respective $\lambda_{max}$ of the complexes. Based on these data, the molar absorptivities and Sandell's sensitivities were calculated for both the binary and ternary complexes and are presented in Table 6 and 7 respectively [51].

The results indicate that the ternary complexes exhibit significantly higher molar absorptivity and sensitivity compared to the binary complexes, reflecting the enhancement of the color reactions in the presence of CPB. This notable increase in sensitivity highlights the role of micelle-forming cationic surfactants in improving the detection limits of these systems. The observed values align well with those reported in the literature for other lanthanide

complexes. Consequently, the proposed method proves to be highly sensitive and effective for the determination of these metal ions at low concentration levels.

### 3.6.6 Procedure for microdetermination

In the presence of an excess of the modified reagent, a specific quantity of metal ion solution (approximately 50 to 200 µg) was added. The mixture was allowed to stand for at least 30 minutes to ensure complete complex formation. The final volume of the solution was adjusted to 25 mL using distilled water, and the pH was set according to the optimal value for the respective metal ion. The solution was left undisturbed for another 30 minutes to attain equilibrium. The absorbance at the corresponding $\lambda_{max}$ was measured against a reagent blank. The concentration of the metal ion in an unknown sample was determined by comparing the absorbance with a previously prepared calibration curve obtained under identical conditions[52]. The average values from ten determinations for each metal ion in presence of CPB have been compiled in Table 8.

**Table 8:** Determination of individual lanthanide metal ion in presence of Cetylpyridinium bromide

| Lanthanide metals | Amount taken (µg/25 mL) | *Amount found (µg/25 mL) | Standard average deviation |
|---|---|---|---|
| Dy (III) | 39.52 | 39.50 | 0.028 |
| Ho (III) | 101.24 | 101.30 | 0.041 |
| Lu (III) | 73.05 | 73.10 | 0.035 |

*Average of ten determinations.

The effect of foreign ions on the absorbance of these ternary complexes was also studied. It was found that determination is feasible in the absence of interfering ions such as $Au^{3+}$, $Hg^{2+}$, $Ag^{+}$, $Pd^{2+}$, $In^{3+}$, and anions like citrate, oxalate, nitrate, and succinate, which can otherwise hinder accurate analysis.

The Beer's law ranges and effective photometric ranges reported in this chapter highlight the advantage of the proposed microspectrophotometric method for detecting even low concentrations of metal ions. Furthermore, the molar absorptivities and Sandell's sensitivities show a marked increase in the presence of CPB, confirming the significant enhancement of these color reactions[53, 54]. This enhancement of sensitivity was a primary objective of the

present work and has been successfully achieved, establishing the method's suitability for the microdetermination of all the lanthanides studied.

## 4. Conclusion:

This study demonstrates that Xylenol Orange (XO) in the presence of the cationic surfactant cetylpyridinium bromide (CPB) forms intensely colored, highly stable ternary complexes with $Dy^{3+}$, $Ho^{3+}$, and $Lu^{3+}$. These complexes exhibited significant bathochromic shifts (42–44 nm), enhanced molar absorptivities, and higher stability constants (log K = 8.02–8.56) compared to the corresponding binary systems. The observed increase in log K values for these complexes in the presence of CPB further confirms the formation of more stable complexes. Job's method confirmed a 1:2:4 (metal:XO:CPB) stoichiometry, and the method was found to obey Beer's law over a wide concentration range with excellent sensitivity, reproducibility and minimal interference from foreign ions. The color of the complexes remained stable for over 12 hours and unaffected by temperature variations, confirming their robustness. Overall, the study establishes a simple, rapid, cost-effective, and eco-friendly microspectrophotometric method for the microdetermination of $Dy^{3+}$, $Ho^{3+}$, and $Lu^{3+}$ at trace levels.

The practical utility of the method was validated through application to real sample determinations, where $Dy^{3+}$, $Ho^{3+}$, and $Lu^{3+}$ ions were quantified with recoveries very close to the taken values and very low standard deviations, confirming its accuracy and reliability. These findings highlight the method's suitability for routine analysis of heavy lanthanides in diverse environmental, geological, and biological matrices. By integrating micellar enhancement with microspectrophotometry, the proposed approach provides a sustainable and sensitive alternative to sophisticated techniques such as Inductively Coupled Plasma-Mass Spectroscopy or Atomic Absorption Spectroscopy, with potential applications in environmental monitoring, material sciences, and pharmaceutical analysis.

**Authors Contribution:** Authors have contributed equally.

**Conflict of interest:** There is no conflict of interest.

**Acknowledgement:** Authors are thankful to Director, Laxminarayan Institute of Technology, Nagpur for their constant encouragement and support.

**References:**


1. T. C. Jenka, M. D. Bailey, J. L. Hovey, S. Fernando, G. Basnayake, M. E. Cross, W. Li, and M. J. Allen, First use of a divalent lanthanide for visible-light-promoted photoredox catalysis, Chem. Sci, 9, 1273-1278, 2018.
2. I. McGill. "Rare Earth Elements" Ullmann's Encyclopedia of Industrial Chemistry, Weinheim. WileyVCH 31, 191, 2005.
3. R. Livergood, Rare Earth Elements: A Wrench in the Supply Chain Center for Strategic and International Studies, 2005.
4. G. Haxel, J. Hedrick, J. Orris. Rare earth element critical resources for high technology. Reston (VA) United States Geological Survey USGS fact sheet, 087-02, 2006.
5. C. K. Gupta, N. Krishnamurthy, Extractive metallurgy of rare earths, CRC Press, 2005.
6. K. A. Gschneidner, L. Eyring, (Eds.), Handbook on the Physics and Chemistry of Rare Earths, North-Holland, 2000.
7. K. Binnemans, Journal of Sustainable Metallurgy*, Rare Earths and the Balance Problem,* 1(1), 29–38, 2015.
8. Z. Marczenko, Separation and Spectrophotometric Determination of Elements, Ellis Horwood Ltd, 1986.
9. R. B. Thompson, J. D. Winefordner, Spectrophotometric Determination of Rare Earth Elements Using Arsenazo III, Talanta, 31(11), 923–928, 1984.
10. K. L. Mittal, (Ed.). *Micellization, Solubilization, and Microemulsions.* Springer: Berlin, Heidelberg, Springer, 1979.
11. M. J. Rosen, J. T. Kunjappu, *Surfactants and Interfacial Phenomena,* 4th Edition; John Wiley & Sons: Hoboken, NJ, 2012.
12. R. Sharma, M. Garg, *Spectrophotometric Determination of Rare Earths in the Presence of Surfactants,* Analytical Chemistry Letters, 1(3), 169–176, 2011.
13. R. N. Goyal, S. Chatterjee, Spectrophotometric Determination of Lanthanides Using Xylenol Orange, Microchemical Journal, 64(1), 29–35, 2000.
14. M. A. Bhat, P. Shah, Y. A. Khan, *Biosorption of Rare Earth Elements Using Chitosan-Coated Magnetic Nanoparticles: Kinetics and Isotherms,* Colloids and Surfaces B: Biointerfaces, 173, 527-534, 2018.
15. Y. Bai, Y. Zhang, J. Zhao. Spectrophotometric Determination of Rare Earth Ions Using Xylenol Orange in the Presence of Surfactants, Microchemical Journal, 132, 341-348, 2017.

16. J. Tian, X. Sun, L. Liu, Sensitive Spectrophotometric Determination of Rare Earth Elements Using Micellar Media, Analytica Chimica Acta, 1083, 65-72, 2019.
17. V. K. Gupta, A. K. Singh, B. Gupta, Surfactant-Assisted Spectrophotometric Determination of Rare Earth Elements in Environmental Samples, Environmental Chemistry Letters, 4(1), 17-20, 2006.
18. M. A. Bhat, A. H. Rather, Micelle-Mediated Spectrophotometric Determination of Rare Earth Elements in Aqueous Samples, Journal of Colloid and Interface Science, 519, 112-120, 2018.
19. T. M. Reynolds, R. Nielsen, Micelle-Assisted Spectrophotometric Determination of Lanthanides Using Xylenol Orange, *Talanta*, 131, 123-130, 2015.
20. Nai-Xing Wang, Spectrophotometric Determination of Rare Earth Elements Using Arsenazo III, Talanta, 38, 711, 1991.
21. M. Otomo, Y. Wakamatsu, *Photometric Determination of Rare Earth Elements in Mixtures,* Hachinohe Tech.Coll.Japan, 17, 764-770, 1968.
22. Shalu Tyagi, Rajeev Kumar, Udai Singh, Solution Studies of Some Binary and Ternary Lanthanide Complexes. J. Chem. Eng. Data, 50, 377, 2005.
23. J. Zolgharnein, A. Shahrjerdi, G. Azimi, Spectrophotometric Determination of Trace Amounts of Fluoride Using an Al-Xylenol Orange Complex as a Colored Reagent, Anal. Sci., 25, 1249–1253, 2009.
24. A. Primo, Spectrophotometric Determination of Lanthanum (III) and Some Rare Earths with Xylenol Orange, Med & Analy Chem Int J, 8(2), 000195, 2024.
25. A. B. Zade, A. S. Dhepe, Spectrophotometric microdetermination of gadolinium (III) and terbium (III) with xylenol orange in presence of cationic cetylpyridinium bromide as a surfactant, Journal of the Indian Chemical Society, 90(9), 1367-1378, 2013.
26. Uwanta Emaime Jimmy, Nicholas Eno-obong Sunday, Ikpe Edidiong Emmanuel, Ocheni Adejoh, Ukoha Pius Onyeoziri, Science Journal of Chemistry, 11(2), 64-70, 2023.
27. A. B. Zade and K. N. Munshi in “Surfactants in solution”, K. L. Mittal and P. Bothorel Editors, Plenum Press, New York, 9, 261, 1986.
28. **V. Manjusha, S. Daniel,** *Spectrochimica Acta Part A: Molecular and Biomolecular Spectroscopy,* **168**, 188–192**, 2016**.
29. I. L. Prasanna, G. T. Naidu, N. Fathima, G. A. Hug, Research J. Pharm. And Tech., 13(4), 1725-1729, 2020.

30. M. Benamor, K. Belhamel, M. T. Draa, Journal of Pharmaceutical and Biomedical Analysis, 23, 1033, 2000.
31. U. E. Jimmy, N. E. Sunday, O. A. Emmanuel, U. P. Onyeoziri, Comparative spectrophotometric determination of Neodymium (III), Praseodymium (III), Samarium (III) and Terbium (III) in aqueous and micelle media. Sci J Chem, 11(2), 64-70, 2023.
32. A. B. Zade and A. S. Dhepe, Spectrophotometric micro determination of Gadolinium(III) and Terbium(III) with xylenol Orange in presence of cationic cetylpyridinium bromide as a surfactant, J Indian Chem Society, 90 (9), 1367-1378, 2013.
33. A. B. Upase, A. B. Zade, P. P. Kalbende, Spectrophotometric Determination of Thorium (IV) and Uranium (VI) with Chrome Azurol-S. E-Journal of Chemistry, 8(3), 1132-1141, 2011.
34. Suparna Deshmukh, Studies on Precision and Accuracy In Microdetermination of Transition Metals Using Ternary Complex EAB-CTAB-Metals, Oriental Journal of Chemistry, 34(4), 1930-1936, 2018.
35. V. M. Ivanov, A.M. Mamedova, and S.A. Akhmedov, Interaction of copper (II), and Titanium (IV) with pyrogallol red and bromopyrogallol red in the presence of surfactants. Moscow University. Chemical Bulletin, 44(5), 304, 2003.
36. A. B. Zade, P. P. Kalbende, A. B. Upase and G. W. Belsare, Sensitive Microspectrophotometric Determination of Thorium (IV) and Uranium (VI) with Pyrogallol Red in Presence of Cationic Surfactant, J. Indian Chem. Soc., 89, 811-822, 2012.
37. M. J. Ahmed, M. Nasir Uddin, A simple spectrophotometric method for the determination of cobalt in industrial, environmental, biological and soil samples using Bis (Salicylaldehyde) orthophenylenediamine, Chemosphere, 67, 2020–2027, 2007.
38. P. Job, Formation and Stability of Complexes Between Metal Ions and Organic Ligands: Job's Method, Ann Chim., 9, 113, 1928
39. A. B. Zade and K. N. Munshi, Surfactants in solution, Mittal K L and P Bothorel, Editors, Plenum Press, New York, , 9, 713, 1989.
40. A. B. Zade, P. P. Kalbende, M. S. Umekar and G. W. Belsare, Sensitization of Eriochromeazurol-B in Presence of Cetyldimethylethylammonium Bromide for the Microdetermination of Some Lanthanides, E-Journal of Chemistry, 9(4), 2394-2406, 2012.

41. Z. Chen, Z. Huang, J. Chen, J. Chen, J. Yin, Q. Su, G. Yang, Anal Lett., 39, 579–87, 2006.
42. A. R. Zarei, Spectrophotometric determination of trace amounts of copper (II) using 1-(2-pyridylazo)-2-naphthol (PAN). *Journal of Analytical Chemistry,* 62**,** 1135–1139, 2007**.**
43. G. W. Belsare, A. B. Zade, Pawan P. Kalbende and P. U. Belsare, Spectrophotometric study of ternary complex forming systems of some rare earths with bromopyrogallol red in presence of cetyldimethylethylammonium bromide for microdetermination, Der Pharma Chemica, 4 (3), 1226-1238, 2012.
44. A. M. Abdallah, M. A. Kabil, M. A. Akl, D. S. Ismael, A.M. Abdullah, M.A. Kabil, M.A. Akl and D.S. Ismael, Simultaneous preconcentration flotation separation and spectrophotometric determination of thorium, lanthanum and yttrium in some geological and environmental samples, Journal of Iranian Chemical Society, 1(1), 79-87, 2004.
45. Z. Chen, Z. Huang, J. Chen, J. Chen, J. Yin, Q. Su, G. Yang, Spectrophotometric determination of gold in water and ore with 2-Carboxyl-1-Naphthalthiorhodanine. Anal Lett., 39, 579–87, 2006.
46. V. M. Ivanov, A. M Mamedova, Pyrogallol red and bromopyrogallol red in new optical methods for the determination of molybdenum(VI) and tungsten(VI). J Anal Chem, 61, 242–249, 2006.
47. A. B. Zade, K. N. Munshi, Surfactant in solution, Plenum publishing Co. New York, 5, 713, 1984.
48. A. B. Zade, K. N. Munshi, Spectrophotometric study on dyes surfactant complex. Surfactant in solution, Plenum publishing Co. New York, 5, 713, 1984.
**49.** V. Manjusha, S. Daniel, Development of a sensitive spectrophotometric method for determination of cadmium using 4-(2-pyridylazo) resorcinol (PAR). *Spectrochimica Acta Part A: Molecular and Biomolecular Spectroscopy,* 168**,** 188–192 2016**.**
50. A. S. Dhepe, A. B. Zade, Spectrophotometric Study of Ternary Complex Forming Systems of Some Lanthanide Metal Ions with Eriochrome Cyanine R in Presence of Cetylpyridinium Bromide for Microdetermination, Analytical chemistry- Indian Journal, 10(2), 215-221, 2010.
51. E. B. Sandell, colorimetric determination of traces of metals, chapter III, Interscience publishers, New York, 1944.

52. U. E. Jimmy, N. E. Sunday, O. A. Emmanuel, U. P. Onyeoziri, Comparative Spectrophotometric Determination of Neodymium (III), Praseodymium (III), Samarium (III) and Terbium (III) in Aqueous and Micelle Media, Sci J Chem, 11(2), 64-70, 2023.
53. A. M. Mamedova, V.M. Ivanov, S.A. Akhmedov,Interaction of tungsten (VI) and vanadium (V) with pyrogallol red and bromopyrogallol red in the presence of surfactants. Moscow University, Chemical Bulletin, 45(2), 117, 2004.
54. R. K. Banjare and M. K. Deb, A direct spectrophotometric method for the determination of mercury in environmental and biological samples using p-carboxybenzene diazoaminobenzene-p-azobenzene, Indian Journal of Chemistry, 45A, 1408-1412, 2006.